SPECIAL TOPIC — Ultracold atom and its application in precision measurement

Study of optical clocks based on ultracold ^{171}Yb atoms*

Di Ai(艾迪)[1], Hao Qiao(谯皓)[1], Shuang Zhang(张爽)[1], Li-Meng Luo(骆莉梦)[1], Chang-Yue Sun(孙常越)[1], Sheng Zhang(张胜)[1], Cheng-Quan Peng(彭成权)[1], Qi-Chao Qi(齐启超)[1], Tao-Yun Jin(金涛韫)[1], Min Zhou(周敏)[1], and Xin-Ye Xu(徐信业)[1,2,†]

[1] *State Key Laboratory of Precision Spectroscopy, East China Normal University, Shanghai* 200062, *China*
[2] *Shanghai Research Center for Quantum Sciences, Shanghai* 201315, *China*

(Received 9 May 2020; revised manuscript received 8 June 2020; accepted manuscript online 29 June 2020)

The optical atomic clocks have the potential to transform global timekeeping, relying on the state-of-the-art accuracy and stability, and greatly improve the measurement precision for a wide range of scientific and technological applications. Herein we report on the development of the optical clock based on ^{171}Yb atoms confined in an optical lattice. A minimum width of 1.92-Hz Rabi spectra has been obtained with a new 578-nm clock interrogation laser. The in-loop fractional instability of the ^{171}Yb clock reaches 9.1×10^{-18} after an averaging over a time of 2.0×10^{4} s. By synchronous comparison between two clocks, we demonstrate that our ^{171}Yb optical lattice clock achieves a fractional instability of $4.60\times10^{-16}/\sqrt{\tau}$.

Keywords: cold ytterbium atoms, optical clocks, ultra-stable clock lasers, clock-transition spectra, instability and uncertainty

PACS: 06.30.Ft, 32.30.–r, 32.70.Jz, 37.10.Jk **DOI:** 10.1088/1674-1056/aba099

1. Introduction

As one of the seven basic international units, the time unit of seconds is widely used in the field of precision metrology. Presently, the definition of SI seconds is achieved by the cesium atomic fountain clock. However, advances in laser cooling and trapping, highly stabilized continuous wave (CW) laser sources, and optical frequency comb technology that allow high accuracy comparison of frequencies ranging from the radio frequency (RF) to the ultra-violet (UV), the latest generation of atomic clocks based on narrow optical transitions in atoms or ions have already demonstrated the ability to measure time or frequency at an unprecedented level.[1–4] Optical lattice clocks, by confining atoms to the Lamb–Dicke regime, have an extremely high optical transition quality factors compared to the ion optical clock,[5] which greatly improves the signal-to-noise ratio of the clock transition.[6,7] State-of-the-art atomic optical clocks have achieved fractional frequency instabilities near $1.5\times10^{-16}/\sqrt{\tau}$ and reached 4.5×10^{-19} after 36 h, systematic uncertainties of a few parts in 10^{-18} level.[8,9] Therefore, the optical atomic clock is expected to become the next generation time and frequency standard.[10–12]

The two most important indicators to evaluate the performance of optical clocks are frequency instability and systematic uncertainty. However, the systematic uncertainty is often constrained by long-term instability, and a better instability can greatly improve the efficiency to evaluate systematic uncertainties.[13,14] In an optical atomic clock, the short-term stability is mainly determined by the ultra-stable clock laser which serves as the local oscillator (LO) while the long-term instability is limited by the Dick effect.[15]

In this paper, we achieve the closed-loop lock of ^{171}Yb optical clock using a new clock laser system. The frequency of clock laser is stabilized to a 30-cm ultra-low-expansion (ULE) cavity. Synchronous frequency comparison between two ^{171}Yb optical clocks is also implemented, determining the single-clock instability of $4.60\times10^{-16}/\sqrt{\tau}$.

2. Experimental setup

For ^{171}Yb, $I=1/2$, the hyperfine structure is relatively simple, and the tensor light shift introduced by the optical lattice is zero. The energy levels and transitions of Yb atoms related to atomic clocks are shown in Fig. 1. Experimental details are similar with our previous works.[16–18] Two independent clock systems labeled as Yb1 and Yb2 cool and trap ^{171}Yb atoms from thermal beams into two-stage magneto optical traps (MOT): first is 399-nm blue MOT for 500 ms, followed by 556-nm green MOT for 100 ms. After that atoms are loaded into a one-dimensional (1D) optical lattice formed by 759-nm Ti:sapphire lasers LL1 and LL2, respectively. The experimental setup is shown as Fig. 2. After obtaining ultra-cold ytterbium atoms in an optical lattice, the next step is to pre-

*Project supported by the National Key Basic Research and Development Program of China (Grant Nos. 2016YFA0302103, 2017YFF0212003, and 2016YFB0501601), the Municipal Science and Technology Major Project of Shanghai, China (Grant No. 2019SHDZX01), the National Natural Science Foundation of China (Grant No. 11134003), and the Excellent Academic Leaders Program of Shanghai, China (Grant No. 12XD1402400).

†Corresponding author. E-mail: xyxu@phy.ecnu.edu.cn

pare them for spectroscopy. Before that, we implement a spin-polarization protocol using 556-nm laser to pump all the atoms to one of the spin-state (either $m_F = 1/2$ or $m_F = -1/2$), which can almost double the spectral contrast excited by the clock laser. Then the clock transition $^1S_0$–$^3P_0$ will be probed with 578-nm laser stabilized to a high-finesse Fabry–Pérot (FP) cavity. Subsequently, we use two re-pumpers at 649 nm and 770 nm to assist most of excited atoms return to the ground state $^1S_0$. Then applying a sequence of three pulses (5 ms each) resonant with the $^1S_0$–$^1P_1$ transition to detect the fraction of excited atoms and collect the fluorescence on a photomultiplier tube (PMT), which will greatly reduce the effect of shot-to-shot atom number fluctuations.

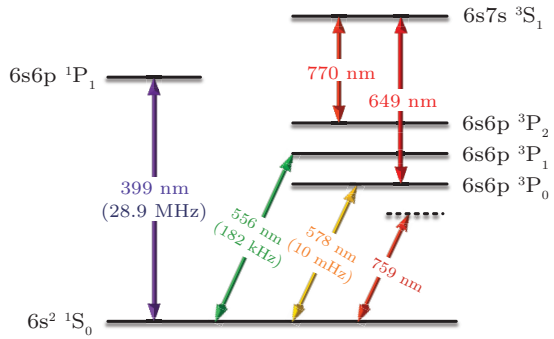

Fig. 1. Relevant energy levels of the ytterbium atomic clock. Lasers for two cooling transitions (399 nm and 556 nm), optical lattice (759 nm), clock transition (578 nm), and two re-pumping transitions (649 nm and 770 nm).

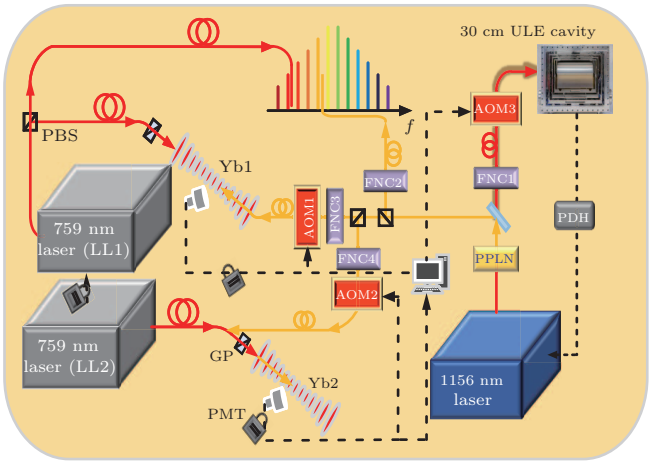

Fig. 2. Schematic diagram of the experimental setup. The 578-nm clock laser is generated by frequency doubling of a 1156-nm laser, and we send part of it to the lattice system for clock interrogation and small part of it to an optical frequency comb for stabilizing the repetition frequency of the comb and measuring the absolute frequency of ^{171}Yb. The frequency of LL1 is locked to the comb, and LL2 is offset locked to LL1. PBS: polarizing beam splitter; FNC: fiber noise cancellation; PMT: photomultiplier; GP: Glan polarizer; PDH: Pound–Drever–Hall.

3. Ultra-stable clock laser

The central component of the stabilized clock laser is a high finesse FP cavity. The 1156-nm semiconductor laser is used as an optical source, which is locked to the ultra-stable FP cavity (see Fig. 3). The cavity is made of ULE glass spacer of 30-cm length and two optically contacted ULE glass mirrors, in which one mirror is planar used as the input coupler and the other has a radius of curvature of 1 m. The cavity finesse at 1156 nm is 295900 (1.7-kHz linewidth), based upon an average of cavity ring-down measurements (CRDS). According to the expression in Refs. [19,20], the fractional frequency instability limit of the clock laser from the thermal noise of the cavity is calculated to be about 2×10^{-16}. The vacuum chamber is actively temperature stabilized, while there are also three aluminium shells with space for thermal insulation between each providing passive stabilization surrounding the vacuum housing. The pressure in the vacuum chamber is maintained at 10^{-9} Torr (1 Torr $= 1.33322 \times 10^2$ Pa).

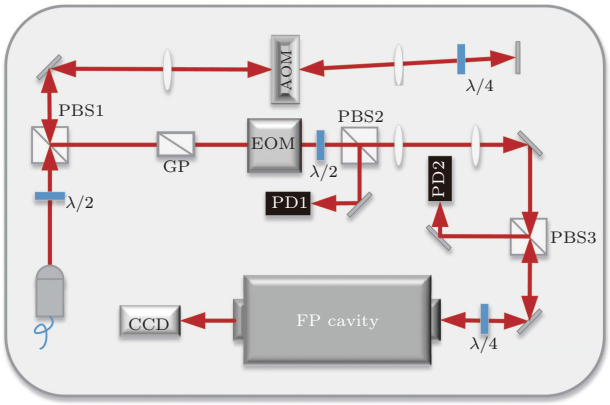

Fig. 3. Simplified experimental setup of 1156-nm ultra-stable laser system. PBS: polarizing beam splitter; PD: photo diode; AOM: acousto–optic modulator; EOM: electro–optic modulator; GP: Glan polarizer; $\lambda/2$: 1/2 waveplate, $\lambda/4$: 1/4 waveplate.

As shown in Fig. 4, the FP cavity is placed on an active vibration platform and inside an acoustic-damping enclosure to prevent the coupling of vibration noise and acoustic noise into the cavity. A 10-m long optical fiber is used to deliver light from the 1156-nm laser table to the FP cavity, and a fiber noise cancelation (FNC1) system is used to eliminate the phase noise introduced by the fiber.[21] The intracavity light heats the mirror coatings, leading to a shift of the cavity resonance about 0.4 Hz/μW.[22] To minimize this effect, we only couple 15 μW of 1156-nm light into the FP cavity. Meanwhile, the 1156-nm input power is stabilized about 0.1% by active controlling the RF driving power of the AOM.

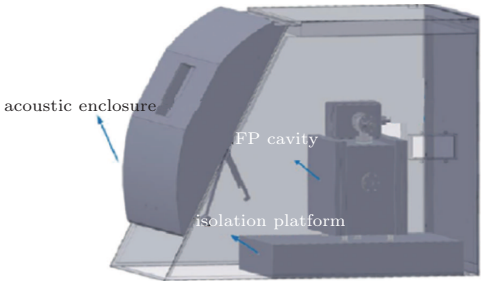

Fig. 4. Sectional view of 1156-nm ultra-stable FP cavity system.

The high-finesse FP cavity not only need to have low sensitivity to temperature variations, but also need to be well protected from environmental perturbations. It is critical to keep

the cavity as close as possible to the zero coefficient of thermal expansion (CTE) temperature, so as to minimize the effects of the temperature T_{cav} variation in cavity on its length.[23] When plotting the 1156-nm laser frequency as a function of the FP cavity temperature T_{cav}, the curve shows the parabolic dependency. From the experimental value, we have determined the temperature at which the coefficient of thermal expansion is zero to be 32.93 °C (see Fig. 5).

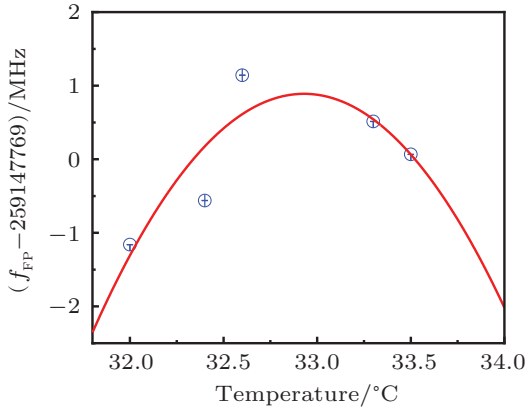

Fig. 5. Determination of the zero coefficient of thermal expansion temperature for the FP cavity. Each data point is measured for different cavity temperatures once the temperature in the vacuum chamber is stable.

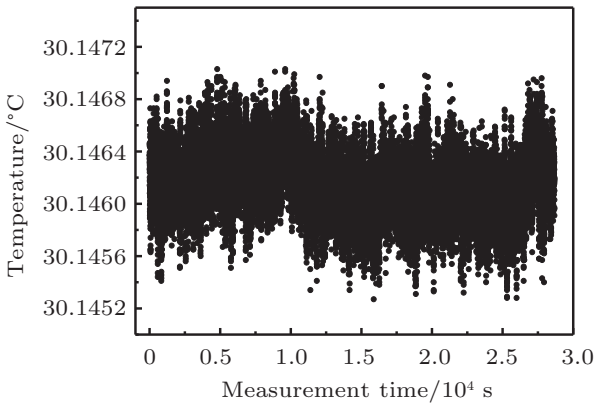

Fig. 6. The temperature fluctuation of EOM under temperature control.

The residual amplitude modulation (RAM) is one of the most important factors that affect the stability of the clock laser locking.[24] In order to reduce the effect of RAM, on the one hand, it is necessary to accurately control the temperature of the electro–optic modulator (EOM) for reducing the impact of the external environment on the EOM. On the other hand, it is necessary to keep the temperature at the point where the RAM is not sensitive to temperature changes. In addition, we use a Glan polarizer with an extinction ratio higher than 10^5 to purify the laser polarization, which will ensure the polarization of the 1156-nm laser can be consistent with the direction of the modulated electric field. In the experiment, we use the thermoelectric cooler (TEC) to control the temperature of EOM, and the long-term fluctuation of temperature is less than 2 mK, as shown in Fig. 6. In order to reduce the influence of ambient temperature fluctuations on the stability of the FP cavity, we surround six TECs around the vacuum chamber. With this temperature control, the temperature fluctuation of the passive shield remains within 5 mK in the room temperature (changes by about 1 K).

We employ the Pound–Drever–Hall (PDH) technology to stabilize the 1156-nm laser to the FP cavity. In our experiment scheme, the PDH error signal is divided into two parts, one part is sent to the piezoelectric transducer (PZT) feedback terminal as slow feedback, which can effectively reduce the influence of slow changing factors such as temperature. And the other is sent to the current feedback terminal as fast feedback, whose servo bandwidth is in the order of megahertz, which can effectively suppress the noise of the laser itself and the noise caused by the external environment, and the slow feedback. Under the joint action of the two feedbacks of the servo system, the frequency of 1156-nm laser is stabilized to FP cavity, thereby obtaining a stable 578-nm laser.

4. Clock transition spectra of ^{171}Yb

With the improved performance of our new 578-nm clock laser, it can coherently excite the clock transition for a longer time, which can obtain a narrower clock transition spectrum. In our experiment, with a Rabi probe time of 600 ms, we obtain the 1.92-Hz linewidth (FWHM) atomic spectra (see Fig. 7), which is slightly wider than the Fourier-limited linewidth of 1.33 Hz ($0.8/t = 1.33$ Hz, t is the probe time of clock interrogation). This is due to the reason that the achievable linewidth of clock transition spectra is limited by various factors in experiment, such as atomic temperature, lifetime of optical lattice, misalignment between the 578-nm clock laser and the 759-nm lattice laser.[25] The 600-ms Rabi probe time could obtain a very narrow atomic spectra, however, which also makes the atom lock sensitive to short-term clock laser frequency excursions. Sometimes it may arouse the frequency shift to exceed the atomic capture range of linewidth of atom spectra and leads to the loss of lock. Therefore, in order to ensure the stability of the lock, we chose to operate the system with a 200-ms probe time.

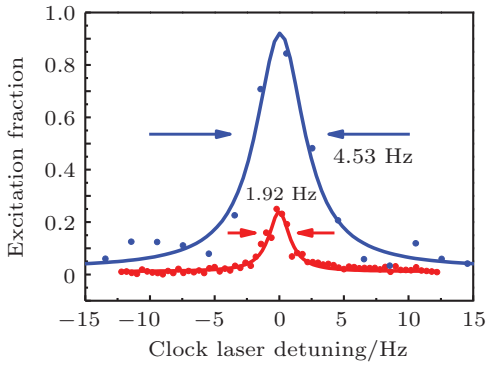

Fig. 7. Normalized clock transition spectra of π component in ^{171}Yb. Blue and red points are the data for interrogation times of 200 ms and 600 ms, respectively. Employing Lorenz fit to the signal produces the FWHM linewidth of 1.92 Hz (red curve) and 4.53 Hz (blue curve).

5. In-loop operation and synchronous frequency comparison

A standard four-point locking procedure is applied in the closed-loop operation of the clock.[16,26] The 578-nm laser alternately interrogates the two π components of the clock transition at each half-maximum point that the central frequencies of the two peaks are separated by 442 Hz with a bias magnetic field of 1.09 Gs (1 Gs $= 10^{-4}$ T). The single characteristic cycle time is 995 ms involving one cooling–interrogation–detection cycle. For the four measurements, the data are treated by the software as atomic servo error signal, which is applied to the bridging AOM1 that completes the feedback control of the clock laser and tunes the frequency on-resonance with the atomic transition. Meanwhile, to further improve the locking robustness, a real-time feedforward by fitting the updating frequency correction of bridging AOM1 is applied to AOM3 to compensate the drift of the clock laser. To check the frequency instability of our clock, the Yb1 clock has operated continuously for more than 4×10^4 s. The result of this measurement is shown as blue points in Fig. 8(b). The in-loop fractional frequency instability of our ^{171}Yb optical lattice clock given by the Allan deviation follows the dependence $1.28 \times 10^{-15}/\sqrt{\tau}$, where τ is the averaging time in seconds. Figure 8 shows that the Allan deviation does not drop smoothly around 3000 s. This may be due to the residual frequency drift of the clock laser, which is not compensated completely. After that, the Allan deviation begins averaging down quickly, and reaches 9.1×10^{-18} at an averaging time of 2×10^4 s. Therefore, to obtain a better instability, it is necessary to improve the stability of the clock laser as much as possible and reduce the irregular drift and jitter of the clock laser frequency. In addition, there is only less than 40% of the cycle time spent on the clock interrogation, which results in augmenting the clock instability (Dick effect). Therefore, it is necessary to reduce the preparation time in the experimental cycle.

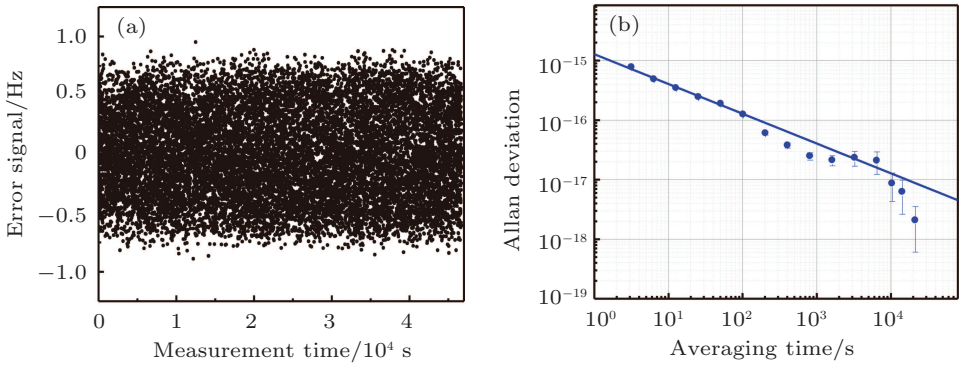

Fig. 8. (a) The in-loop error signal. (b) Instability evaluation of the ytterbium clock using the atomic transition. Blue points give the in-loop instability (from the error signals) when the 578-nm laser is locked to the atomic transition, and the blue line shows an instability of $1.28 \times 10^{-15}/\sqrt{\tau}$.

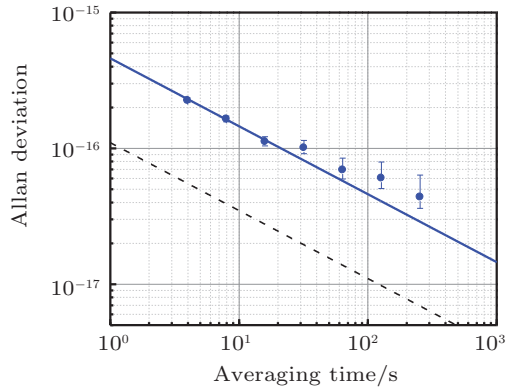

Fig. 9. Single clock stability measured with a synchronous comparison between two ^{171}Yb optical lattice clocks. The blue line indicates the measured instability of a single system is $4.60 \times 10^{-16}/\sqrt{\tau}$. The black line shows the quantum projection noise (QNC) limit as $1.1 \times 10^{-16}/\sqrt{\tau}$.

To rigorously assess clock instability, it must be compared to another standard with even lower instability. In our experiment, synchronous frequency comparison is operated between two ^{171}Yb optical clocks that share the same clock laser, which has the potential to cancel out the clock laser frequency noise. Taking this approach, the resulting synchronized measurement instability is shown in Fig. 9, averaging down as $4.60 \times 10^{-16}/\sqrt{\tau}$.

6. Conclusion and perspectives

In conclusion, we have developed a pair of ^{171}Yb optical lattice clocks and completed an improved systematic evaluation based on the new generation clock laser. With the new 578-nm clock interrogation laser, a minimum width of 1.92-Hz Rabi spectra has been obtained with 600-ms interrogation time, and the in-loop fractional instability of closed-loop operation of the ^{171}Yb clock reaches 9.1×10^{-18} after an averaging over a time of 2×10^4 s. Meanwhile, by synchronous comparison between two clocks, we have achieved the fractional instability of a single system assessed to $4.60 \times 10^{-16}/\sqrt{\tau}$. With further improvements of our clock laser and ^{171}Yb lattice systems, we believe that the instability and uncertainty of our clocks will reach to a new level, opening the door to 10^{-18}-level timekeeping precision.

References

[1] Chou C W, Hume D B, Koelemeij J C J, Wineland D J and Rosenband T 2010 *Phys. Rev. Lett.* **104** 070802

[2] Takamoto M, Takano T and Katori H 2011 *Nat. Photon.* **5** 288

[3] Ushijima I, Takamoto M, Das M, Ohkubo T and Katori H 2015 *Nat. Photon.* **9** 185

[4] Huntemann N, Sanner C, Lipphardt B, Tamm Chr and Peik E 2016 *Phys. Rev. Lett.* **116** 063001

[5] Boyd M M, Zelevinsky T, Ludlow A D, Foreman S M, Blatt S, Ido T and Ye J 2006 *Science* **314** 1430

[6] Takamoto M, Pal'chikov V G, Ovsiannikov V D and Katori H 2003 *Phys. Rev. Lett.* **91** 173005

[7] Takamoto M, Hong F L, Higashi R and Katori H 2005 *Nature* **435** 321

[8] McGrew W F, Zhang X, Fasano R J, Schäffer S A, Beloy K, Nicolodi D, Brown R C, Hinkley N, Milani G, Schioppo M, Yoon T H and Ludlow A D 2018 *Nature* **564** 87

[9] Marti G E, Hutson R B, Goban A, Campbell S L, Poli N and Ye J 2018 *Phys. Rev. Lett.* **120** 103201

[10] Riehle and Fritz 2015 *CR Phys.* **16** 506

[11] Targat R Le, Lorini L, Coq Y Le, Zawada M, Guena J, Abgrall M, Gurov M, Rosenbusch P, Rovera D G, Nagorny B, Gartman R, Westergaard P G, Tobar M E, Lours M, Santarelli G, Clairon A, Bize S, Laurent P, Lemonde P and Lodewyck J 2013 *Nat. Commun.* **4** 2109

[12] Margolis H S and Gill P 2015 *Metrologia* **52** 628

[13] Bloom B J, Nicholson T L, Williams J R, Campbell S L, Bishof M, Zhang X, Zhang W, Bromley S L and Ye J 2014 *Nature* **506** 71

[14] Grebing C, Al-Masoudi A, Dorscher S, Hafner S, Gerginov V, Weyers S, Lipphardt B, Riehle F, Sterr U and Lisdat C 2016 *Optica* **3** 563

[15] Quessada A, Kovacich R P, Courtillot I, Clairon A, Santarelli G and Lemonde P 2003 *J. Opt. B: Quantum Semiclass. Opt.* **5** S150

[16] Gao Q, Zhou M, Han C Y, Li S Y, Zhang S, Yao Y, Li B, Qiao H, Ai D, Lou G, Zhang M Y, Jiang Y Y, Bi Z Y, Ma L S and Xu X Y 2018 *Sci. Rep.* **8** 8022

[17] Zhang X H, Zhou M, Chen N, Gao Q, Han C Y, Yao Y, Xu P, Li S Y, Xu Y L, Jiang Y Y, Bi Z Y, Ma L S and Xu X Y 2015 *Laser Phys. Lett.* **12** 025501

[18] Chen N, Zhou M, Chen H Q, Fang S, Huang L Y, Zhang X H, Gao Q, Jiang Y Y, Bi Z Y, Ma L S and Xu X Y 2013 *Chin. Phys. B* **22** 090601

[19] Jiang Y Y, Ludlow A D, Lemke N D, Fox R W, Sherman J A, Ma L S and Oates C W 2011 *Nat. Photon.* **5** 158

[20] Numata K, Kemery A and Camp J 2004 *Phys. Rev. Lett.* **93** 250602

[21] Rauf B, Vélez López M C, Thoumany P, Pizzocaro M and Calonico D 2018 *Rev. Sci. Instrum.* **89** 033103

[22] Young B C, Cruz F C, Itano W M and Bergquist J C 1999 *Phys. Rev. Lett.* **82** 3799

[23] Hagemann C, Grebing C, Lisdat C, Falke S, Legero T, Sterr U, Riehle F, Martin M J and Ye J 2014 *Opt. Lett.* **39** 5102

[24] Black E D 2000 *Am. J. Phys.* **69** 79

[25] Blatt S, Thomsen J W, Campbell G K, Ludlow A D, Swallows M D, Martin M J, Boyd M M and Ye J 2009 *Phys. Rev. A* **80** 052703

[26] Liu H, Zhang X, Jiang K L, Wang J Q, Zhu Q, Xiong Z X, He L X and Lyu B L 2017 *Chin. Phys. Lett.* **34** 020601